

# Design of a Scheffler Mosaic Mirror by Optical Raytracing and CAD Software

Paola Sansoni<sup>1</sup>[\[https://orcid.org/0000-0003-0025-1072\]](https://orcid.org/0000-0003-0025-1072), Daniela Fontani<sup>1</sup>[\[http://orcid.org/0000-0001-5584-1163\]](http://orcid.org/0000-0001-5584-1163), Franco Francini<sup>1</sup>[\[http://orcid.org/0000-0001-7913-4498\]](http://orcid.org/0000-0001-7913-4498), Francesco Toni<sup>1</sup>[\[http://orcid.org/0000-0002-1674-6961\]](http://orcid.org/0000-0002-1674-6961), and David Jafrancesco<sup>1</sup>[\[http://orcid.org/0000-0003-4015-0364\]](http://orcid.org/0000-0003-4015-0364)

<sup>1</sup> CNR National Institute of Optics, Italy

**Abstract.** The Scheffler reflector is a parabolic metal concentrator, typically applied in solar thermal systems with receiver fixed to the ground. The Scheffler mirror is deformed during the year to optimize its solar light collection. For practical reasons it is useful to manufacture such a curve reflector as mosaic mirror. This study develops a configuration of the mosaic mirror type starting from the continuous mirror, trying to indicate how the reflector can be designed. Combining a CAD software tool with raytracing simulations, the optical performance of the Scheffler mosaic mirror is compared with a continuous Scheffler collector. The CAD software reproduces the mechanical deformations of a real Scheffler reflector; while the raytracing software simulates the image that the Scheffler reflector concentrates on the receiver. However, the characteristics of the final composed reflector must be revised depending on the receiver requirements. Moreover, the sizing of the elementary mirrors must be chosen considering the final receiver and it also depends on economic considerations.

**Keywords:** Scheffler Concentrator, Raytracing, CAD Simulations

## 1. Introduction

The main objective of a Scheffler system is to concentrate the light spot produced by a parabolic concentrator on a fixed receiver locked to the ground. This effect is achieved by periodically changing the orientation and profile of a paraboloid calculated for the day of the Equinox [1-2]. There are various articles discussing how to design and build Scheffler mirrors, for the geometric-mechanical aspects [3-4] or considering the mathematical approach [5]. Some examples of applications could be found in the literature, especially for desalination purposes, solar cooking, agriculture [6], and to produce electricity [7,8]. In a recently published article [9], we have indicated the phases for the optical design of the system considering the deformations that must be implemented in order to be able to use only one parabolic concentrator during the year. These phases are: 1. The ideal paraboloid for the equinox is calculated and this will be the parabolic concentrator, which will be deformed over the course of the year. 2. Calculate the ideal paraboloid for the day whose deformations you want to see, for example one of the two solstices. 3. The equinoctial paraboloid is rotated until it overlaps with those calculated in point (2). 4. The rotated equinoctial paraboloid is then deformed so that it can adhere to the ideal one, taking into account the mechanics of its construction.

The concentrator profiles obtained by means of a 3D CAD program are then inserted into an optical software and the irradiance maps are obtained on the receiver. In this way it is possible to evaluate the effect of the deformations on the beam concentrated on the receiver. In the previous study [9] the reflecting surface was of the continuous type, while for the realization of very large mirrors a mosaic type configuration is used. In a mosaic configuration the

mirroring surface is made through the use of many small flat mirrors that are placed in such a way as to follow the shape of the continuous mirror designed, in the examined case a parabolic profile. In this article, therefore, we will study the development of a configuration of the mosaic mirror type starting from the continuous parabolic mirror, trying to indicate how the reflector is designed. Nevertheless, the characteristics of the final composed reflector must be adjusted depending on requirements and features of the effective receiver. The sizing of the elementary mirrors must take into account receiver requirements and economic considerations, which are beyond the scope of this article.

## 2. The design of a parabolic mosaic mirror

The need to switch from a continuous mirror to a mosaic type is mainly due to two factors, the difficulty of making the reflector, especially when the concentrator reaches certain dimensions, and in the case of the Scheffler mirror, the need to deform it during the year to be able to focus the image on the receiver. With large concentrators it may be difficult to achieve the required deformations.

### Dish

For parabolic mirrors generated by rotation and with focus in the rotation axis of the parabola, a general principle is that the smaller the size of the elementary mirrors the better the approximation of the designed profile, however too many elementary mirrors complicate the assembly work and require more complicated structures to manage. In a previous study [9], the concentrator analyzed was composed of a single continuous mirror. However, it should be noted that in many applications the mirror is made with a series of elementary mirrors, all with the same size. This configuration is called mosaic mirror. The dimension of the elementary mirrors affects in various ways the image produced by the reflector. Firstly, smaller is the dimension of the elementary mirror and the continuous mirror is better fitted. Another effect is that the dimension of the elementary mirror also influences the size of the image on the target. In any case, the choice of the dimensions of the elementary mirrors depends mainly on the dimensions  $D_r$  of the receiver and its distance from the mirror  $L$ .

In fact, if  $D_m$  is the dimension of the elementary mirror,  $D_r$  is the receiver aperture,  $L$  the distance between the receiver and the collector,  $\varphi$  the solar divergence, the maximum elementary mirror dimension ( $D_{mMax}$ ) could be roughly estimated as

$$D_{mMax} = D_r - L * 2 \tan(\varphi) \quad (1)$$

Eq. (1) provides a general indication for obtaining the value of  $D_m$  and usually works well for mirrors that have focus on the rotation axis of the paraboloid. A more accurate value will only be obtained with a specific study and with the help of a raytracing program that will also take into consideration the way in which the contributions of the individual faces of the mirror overlap. In fact, the different arrangement of the elementary mirrors also determines the shape of the light spot on the receiver. The use of a 3D CAD program facilitates the design of a mosaic mirror as in the following examples in which we followed two different methods for inserting the mirrors on the parabolic Dish surface.

Method A) A paraboloid is drawn, known its diameter and focal length. The elementary mirrors are arranged according to height curves, which are curves resulting from the section with planes perpendicular to the axis of rotation of the paraboloid. The mirrors are placed with radial symmetry so as to occupy as much space as possible and are increasing in number as the height of the section increases, considering the vertex of the paraboloid as origin. Figure 1 highlights a parabolic surface and a series of elementary mirrors resting on this surface along its height curves. To verify the image produced by the mirror made up of elementary mirrors,

the result of the mechanical design is exported and imported into a raytracing program (Optic-Studio Zemax) with which the irradiance map is obtained on a receiver. Figure 1 represents a mosaic mirror of 171 mirrors resting on a paraboloid with focal length  $f = 1443$  mm. Each elementary mirror has the shape of a square of 150mm x 150mm (diagonal 212mm).

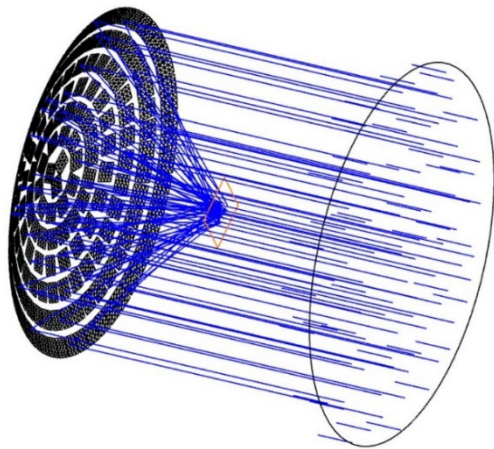


**Figure 1.** Parabolic reflector composed of 171 square mirrors of 150 mm x 150 mm

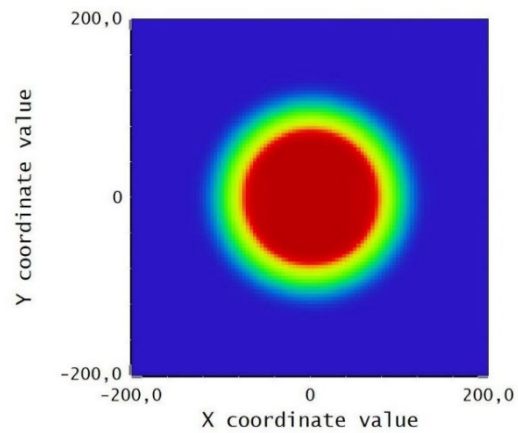


**Figure 2.** Irradiance map on a 400mm square receiver, highlighted in orange in Figure 1

Figures 2 show the irradiance map on a 400mmx400mm square receiver, and the section obtained for  $y = 0$ . The map was obtained with a source with a divergence of  $0.27^\circ$ , in order to simulate the effects of solar lighting. The mid-height spot size is 178mm. The shape of the spot is circular thanks to the radial arrangement of the mirrors.

Method B) The second design mode arranges the mirrors along the intersections of planes parallel to the axis of the paraboloid, parallel to each other and equally spaced, as in Figure 3. The irradiance map on the receiver changes shape and assumes a quadrangular aspect, as Fig4 shows.

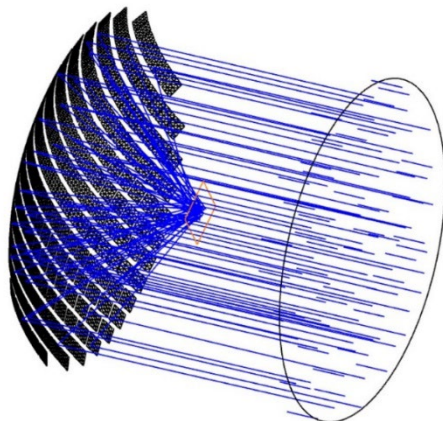


**Figure 3.** Parabolic reflector composed of 190 square mirrors of 150 mm x 150 mm

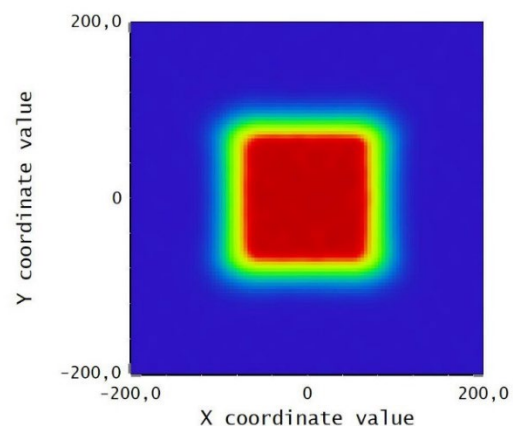


**Figure 4.** Irradiance map on a 400mmx400mm receiver, highlighted in orange in Figure 3.

The advantage of this method is to optimize the space occupied in the positioning of the elementary mirrors and thus increase the mirrored surface. In this case the spot is square because the mirrors are parallel to each other, and the various contributions simply overlap.

## Scheffler reflector

The Scheffler concentrator is the result of a section of the rotation parabola with a cylinder with the axis parallel to that of the parabola, but with the cylinder axis not coinciding with the rotation axis of the parabola. The major difference with respect to the previous cases applied to the Dishes is that these are maintained with the input aperture and the receiver normal to the source. Instead with the Scheffler reflector both the source and the receiver are inclined with respect to the input surface of the paraboloid as shown in Figure 5. The sun's rays are indicated in red, the input surface of the paraboloid is highlighted in green, and the receiver is schematized by the segment in black.

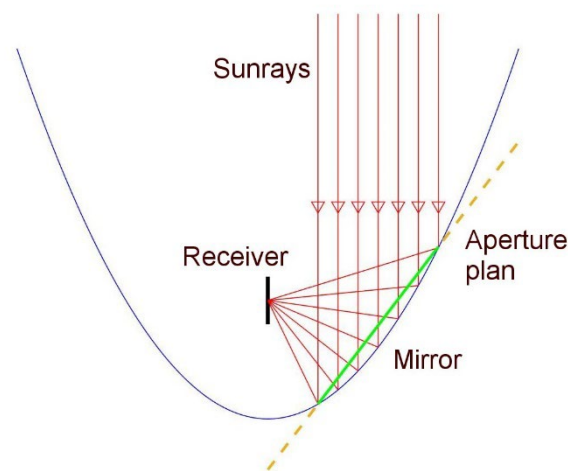


**Figure 5.** Diagram of a Scheffler system: the input surface of the portion of the parabola used (highlighted in green) is not normal to the source nor to the opening of the receiver.

For a Scheffler-type system, the realization of the configuration must be well studied because the paraboloid must be deformed. Furthermore, the construction of the frame is a crucial factor for this type of concentrator because it determines the cost. The frame consists of the crossbars where the elementary mirrors are mounted. The crossbars indicated by Munir et al. [10], are obtained from the intersection with planes normal to the entrance surface of the concentrator and should be of an elliptical shape by construction. This makes them difficult to make. To overcome this difficulty, Munir creates circular crossbars that approximate the elliptical section in 3 points: in the two edges and in the central support [10]. Even if they are easier to produce and at a lower cost, a geometric error is introduced in the reflector. D.S. Reddy and M.K. Khan [5] have introduced a method that involves the construction of crossbars obtained from the intersection of the examined paraboloid with circumferences lying on planes perpendicular to its axis of rotation. This is in fact the application of Method A previously reported. These curves have the advantage of being easy to make and at the same time faithfully following the profile of the paraboloid without introducing approximations, since they are circular by construction. Figure 6 shows the procedure using circumferences (highlighted in blue) with an increasing radius with respect to the plane containing the vertex of the generating parabola, highlighted in magenta.

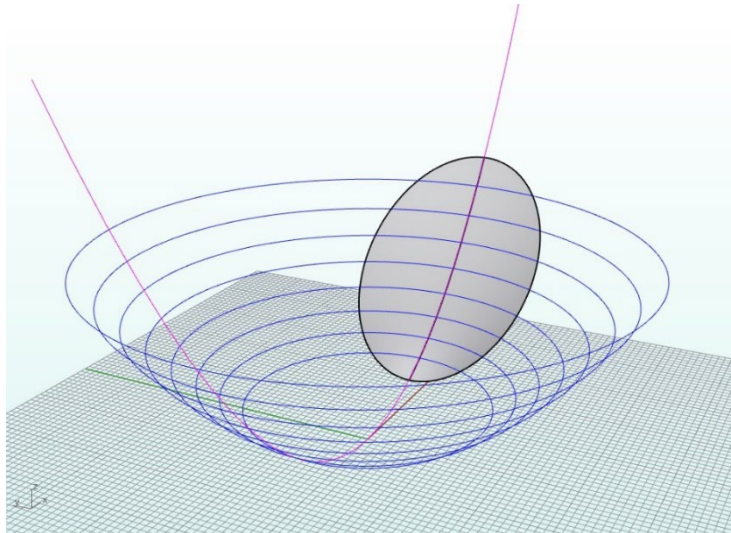


**Figure 6.** Positioning of the crossbars according to the method described by Reddy et al. [5]

The resulting reflector (MM1) is shown in Figure 7. The elementary mirrors were placed within the area occupied by the continuous mirror. Even if we tried to minimize the space between the elementary mirrors, the actual reflecting area of the mirrored reflector is less than the continuous case,  $6.71 \text{ m}^2$ . This must be taken into account for the power calculations.

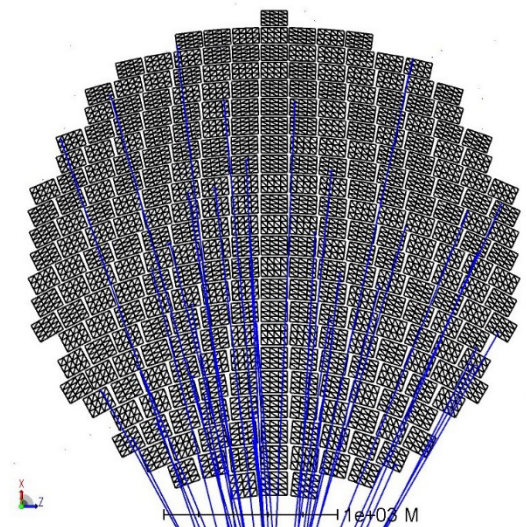


**Figure 7.** Mosaic Mirror (MM1) obtained with the procedure suggested by Reddy et al. [5]. The reflector is made up of square mirrors of  $150\text{mm} \times 150\text{mm}$  resting on a frame having the geometric profile of the equinoctial paraboloid (298 mirrors). View from the source side.

### 3. Comparison of Reflectors

For the comparison we use the irradiance maps obtained for the continuous paraboloid as described in the article and visible in Figures 8-10.

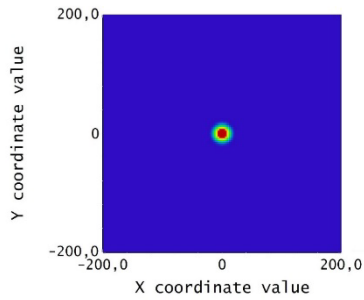


**Figure 8.** Irradiance map of continuous mirror on the receiver on the day of the Equinox.

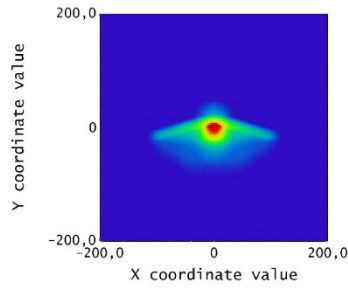


**Figure 9.** Irradiance map of continuous mirror on the receiver on the day of the Summer Solstice.

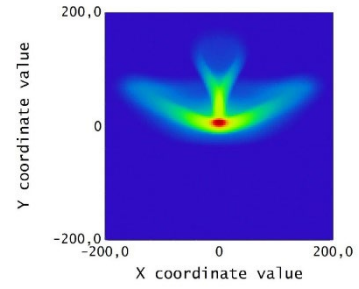


**Figure 10.** Irradiance map of continuous mirror on the receiver on the day of the Winter Solstice.

The Mosaic Mirror MM1 used for the simulations is the one shown in Figure 7 consisting of 293 square-shaped flat mirrors with dimensions of 150mm x 150mm. The relative irradiance maps of the image on the receiver are visible in Figures 11-13.

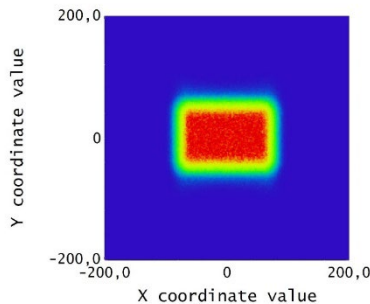


**Figure 11.** Irradiance map of the Mosaic Mirror MM1 made with 150mmx150mm mirrors calculated for the Equinox.

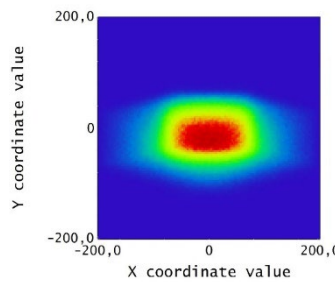


**Figure 12.** Irradiance map of MM1 calculated for the Summer Solstice.

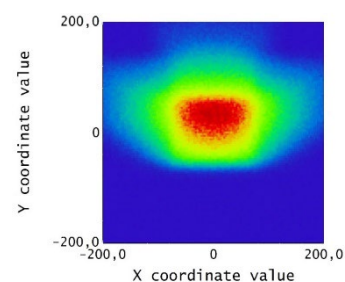


**Figure 13.** Irradiance map of MM1 calculated for the Winter Solstice.

Since the reflectors that have been used as a basis for the calculation are the same as in article of ref. [9], the figures obtained for the mosaic mirror maintain the structure of those obtained with the continuous mirror. The images show some differences, with the formation of 2 lateral structures around the central red spot in the image of the Summer Solstice and 3 lateral structures in the image of the Winter Solstice.

The reason of the rectangular form of the basic image, the one obtained at the equinox, is well explained by Figure 7, where the concentrator is shown from the point of view of the sun. The elementary mirrors are tilted and are seen as rectangles.

A characteristic of the Scheffler configuration, other than the deformations of the reflector, is to be rotated with constant speed during the day to follow the daily movement of the sun. So, the image that is shown in the irradiance map and is relative to noon (see Figure 11), remains the same during the day, but rotates around its center if the receiver is well positioned. It is understood how having a rectangular profile on the best day such as that of the equinox means that a receiver of any shape cannot be uniformly illuminated without losses or the use of a secondary optics. It would therefore be better if the mosaic mirror produced a square image.

Analyzing the profiles of the image obtained for the Equinox for MM1 (Fig. 11), it can be seen that the amplitude ratio is about 1.5. It was therefore decided to create a new mosaic mirror (denominated MM2) with rectangular elementary mirrors measuring 100mm x 150mm. The resulting reflector MM2 is made up of 398 mirrors for a total mirrored area of 5.97 m<sup>2</sup>. The results of the simulations for MM2 are shown in the Figures 14-16: they display the irradiance maps on the receiver for the Equinox and the two Solstices, analogously to Figures 11-13. Comparing Fig. 11 with Fig. 14, corresponding to the Equinox, it can be noted that the image core of Fig. 14 is squared and smaller than the image core of Fig. 11. Analogously, comparing Fig. 12 with Fig. 15, for the Summer Solstice, and comparing Fig. 13 with Fig. 16, for the Winter Solstice, it appears that the image core is more squared and smaller for MM2.

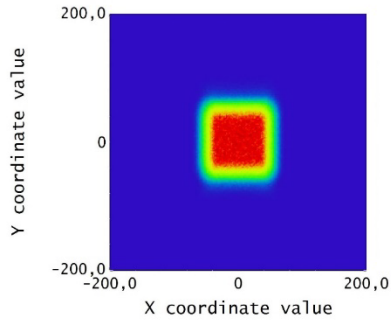


**Figure 14.** Irradiance map of the Mosaic Mirror MM2 with rectangular mirrors measuring 100x150mm at the Equinox.

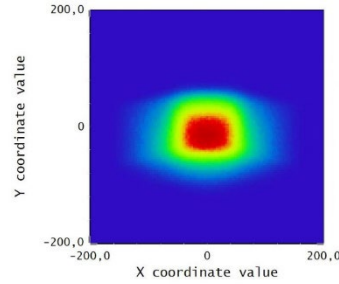


**Figure 15.** Irradiance map of MM2 at the Summer Solstice.

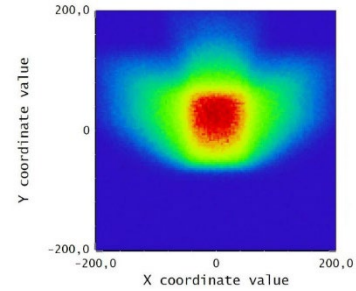


**Figure 16.** Irradiance map of MM2 at the Winter Solstice.

It is also interesting to consider the power collected in the various configurations.

In Table 1 the comparison is made between configurations that have the same reflecting surface of the continuous case, while the concentrators used in the simulations maintain the dimensions of the continuous paraboloid. The results were scaled considering the real reflective area of the concentrators used. It is obvious that in order to reach the same reflecting surface area, real mosaic mirrors will be larger than the continuous mirror, but how to vary the dimensions of the final concentrator depends on the construction and characteristics of the receiver.

**Table 1.** Comparison between the power concentrated by a continuous mirror, the power concentrated by the mosaic mirrors with the same total mirror area (8.28 m<sup>2</sup>).

	<b>Power concentrated by a Continuous Mirror (KWatts)</b>	<b>Power concentrated by a Mosaic Mirror (MM1) with square elementary mirrors (KWatts)</b>	<b>Power concentrated by a Mosaic Mirror (MM2) with rectangular elementary mirrors (KWatts)</b>
Equinox	5,90	5,79	5,65
Summer solstice	4,66	4,67	4,62
Winter solstice	6,89	6,72	6,69

## 4. Conclusions

In this paper it is proposed a study to design a Scheffler-type mosaic mirror employing commercial raytracing software. Combining CAD3D results with raytracing simulations, this study

calculates the light distribution created on the acceptance plane of the receiver by a Mosaic Mirror based on the Scheffler reflector. The working principle of a Scheffler concentrator is based on the local curvature and deformations of the reflector during the year.

The present study has shown that for a non-standard concentrator such as the Scheffler type it is important a collaboration between optical simulation and mechanical simulation to determine the characteristics of the concentrator. The combination of the results of these two software types is fundamental to take into account the mechanical deformations of the Scheffler mirror, during the year. In particular to predict what will be the power and the spot generated by the concentrator on the receiver.

This study presents two possible realizations of mosaic mirrors, starting from the same continuous reflector. These two examples show how the characteristics of the image generated by the mosaic mirror on the receiver depend also on the dimensions and number of the elementary mirrors composing the mosaic mirror. By a practical point of view, it is important to note that the features of the final composed reflector must be adjusted considering the receiver requirements. If uniform lighting is required during the day and throughout the year, it will be necessary to introduce a secondary optic.

Another essential aspect of the functioning of the Scheffler mirror is that during the day the reflector is rotated, so the image also rotates around the center of the receiver. For this reason, probably the solution with a squared image, such that obtained using the MM2 configuration, could be better with respect to the MM1 configuration.

## Data availability statement

The article is based on simulations that anyone can perform following the methodology of the article and there is no data from measurements. The results of this study are not stored in a data repository, so they are not available on the internet. It is a study on the Scheffler reflectors without funding and without research project.

## Author contributions

Author Contributions: Conceptualization, F.F., and D.F.; methodology, F.F., F.T. and D.F.; software, F.T.; validation, P.S.; resources, D.J.; writing—original draft preparation, F.F.; writing—review and editing, P.S.; visualization, D.F.; supervision, D.J. All authors have read and agreed to the published version of the manuscript.

## Competing interests

The authors declare no competing interests.

## Funding

This research received no external funding.

## References

1. U. Oelher, W. Scheffler. The use of indigenous materials for solar conversion. *Solar Energy Materials and Solar Cells* 33 (1994) 379-387. [https://doi.org/10.1016/0927-0248\(94\)90239-9](https://doi.org/10.1016/0927-0248(94)90239-9)

2. W. Scheffler, S. Bruecke, and G. von Werdenbergstr. Introduction to the revolutionary design of Scheffler reflectors. 6th International Conference on Solar Cookers, Granada, Spain. 2006.
3. P. S. Bhambare and S.C. Vishweshwara. Design aspects of a fixed focus type Scheffler concentrator and its receiver for its utilization in thermal processing units. *Energy Nexus* 7 (2022) 100103. <https://doi.org/10.1016/j.nexus.2022.100103>.
4. J. Ruelas, N. Velasques, R. Beltran. Opto–geometric performance of fixed-focus solar concentrators. *Solar Energy*, 141 (2017) 303-310. <https://doi.org/10.1016/j.solener.2016.11.040>
5. D.S. Reddy and M.K. Khan. Design and ray tracing of multifaceted Scheffler reflector with novel crossbars. *Solar Energy* 185 (2019) 363-373. <https://doi.org/10.1016/j.solener.2019.04.083>
6. A. Munir, O. Hensel, W. Scheffler, H. Hoedt, W. Amjad and A. Ghafoor. 2014. Design, Development and Experimental Results of a Solar Distillery for the Essential Oils Extraction from Medicinal and Aromatic Plants. *Solar Energy* 108: 548-559. <https://doi.org/10.1016/j.solener.2014.07.028>
7. H. Panchal, J. Patel, K. Parmar and M. Patel. Different applications of Scheffler reflector for renewable energy: a comprehensive review. *International journal of ambient energy*. Vol. 41, issue 6, 2020. <https://doi.org/10.1080/01430750.2018.1472655>.
8. Q.U Islam and F. Khozaei. The Review of Studies on Scheffler Solar Reflectors. March 2020. Chapter. In book: *Intelligent Techniques and Applications in Science and Technology* (pp.589-595). [https://doi.org/10.1007/978-3-030-42363-6\\_69](https://doi.org/10.1007/978-3-030-42363-6_69).
9. D. Fontani, P. Sansoni, F. Francini, F. Toni, D. Jafrancesco. Optical Raytracing Analysis of a Scheffler Type Concentrator. *Energies* 15 (2022) 260. <https://doi.org/10.3390/en15010260>.
10. A. Munir, O. Hensel and W. Scheffler. Design principle and calculations of a Scheffler fixed focus concentrator for medium temperature applications. *Sol. Energy* 2010, 84, 1490-1502. <https://doi.org/10.1016/j.solener.2010.05.011>